International Journal of Radiation Oncology biology • physics

www.redjournal.org

Physics Contribution

# Intrafraction Prostate Translations and Rotations During Hypofractionated Robotic Radiation Surgery: Dosimetric Impact of Correction Strategies and Margins

**Steven van de Water, MSc,* Lorella Valli, MSc,*,† Shafak Aluwini, MD,* Nico Lanconelli, PhD,† Ben Heijmen, PhD,* and Mischa Hoogeman, PhD***

**Erasmus MC Cancer Institute, Department of Radiation Oncology, Rotterdam, The Netherlands; and †Alma Mater Studiorum, Department of Physics and Astronomy, Bologna University, Bologna, Italy*

Received Oct 16, 2013, and in revised form Dec 22, 2013. Accepted for publication Dec 27, 2013.

**Summary**

A dosimetric evaluation of intrafraction motion was performed for hypofractionated CyberKnife prostate treatments, with a simultaneously integrated boost. Prostate motion was found to have a substantial impact on the delivered dose, but this could be compensated effectively by performing robot corrections using a time interval of 60 to 180 seconds between corrections. A 0-mm planning target volume margin resulted in considerably lower rectum and bladder doses but required larger rotational corrections than a 3-mm margin.

**Purpose:** To investigate the dosimetric impact of intrafraction prostate motion and the effect of robot correction strategies for hypofractionated CyberKnife treatments with a simultaneously integrated boost.

**Methods and Materials:** A total of 548 real-time prostate motion tracks from 17 patients were available for dosimetric simulations of CyberKnife treatments, in which various correction strategies were included. Fixed time intervals between imaging/correction (15, 60, 180, and 360 seconds) were simulated, as well as adaptive timing (ie, the time interval reduced from 60 to 15 seconds in case prostate motion exceeded 3 mm or 2° in consecutive images). The simulated extent of robot corrections was also varied: no corrections, translational corrections only, and translational corrections combined with rotational corrections up to 5°, 10°, and perfect rotational correction. The correction strategies were evaluated for treatment plans with a 0-mm or 3-mm margin around the clinical target volume (CTV). We recorded CTV coverage ($V_{100\%}$) and dose-volume parameters of the peripheral zone (boost), rectum, bladder, and urethra.

**Results:** Planned dose parameters were increasingly preserved with larger extents of robot corrections. A time interval between corrections of 60 to 180 seconds provided optimal preservation of CTV coverage. To achieve 98% CTV coverage in 98% of the treatments, translational and rotational corrections up to 10° were required for the 0-mm margin plans, whereas translational and rotational corrections up to 5° were required for the 3-mm margin plans. Rectum and bladder were spared considerably better in the 0-mm margin plans. Adaptive timing did not improve delivered dose.

**Conclusions:** Intrafraction prostate motion substantially affected the delivered dose but was compensated for effectively by robot corrections using a time interval of 60 to 180 seconds. A 0-mm margin required larger extents of additional rotational corrections than a 3-mm margin but resulted in lower doses to rectum and bladder. 

Reprint requests to: Steven van de Water, MSc, Groene Hilledijk 301, 3075 EA Rotterdam, The Netherlands. Tel: (31) 10 7041111; E-mail: s.vandewater@erasmusmc.nl

Conflict of interest: Erasmus MC Cancer Institute has a research collaboration with Accuray Inc.

Steven van de Water and Lorella Valli contributed equally to this work.

Supplementary material for this article can be found at www.redjournal.org.

*Acknowledgments*—The authors would like to thank Katja Langen for sharing the prostate motion data set.

Int J Radiation Oncol Biol Phys, Vol. 88, No. 5, pp. 1154–1160, 2014
0360-3016/$ - see front matter 
http://dx.doi.org/10.1016/j.ijrobp.2013.12.045

## Introduction

The mobility of the prostate has long since been recognized as a potential source of error during radiation therapy for prostate cancer patients. Several studies have described the characteristics of prostate motion between treatment fractions (1-3). More recently, with the advancement of prostate monitoring techniques, studies have investigated prostate motion during treatment fractions (4-10). For conventional treatment regimens (ie, homogeneous target doses in 2-Gy fractions), the effect of intrafraction prostate motion has been addressed in previous studies (11, 12). Moreover, a technique to perform intrafraction corrections has been implemented clinically by Mutanga et al (13).

The low $\alpha/\beta$ ratio of prostate cancer has triggered a growing interest in the application of hypofractionated radiation therapy for prostate cancer. One of the most extreme hypofractionation regimens currently applied aims at delivering 4 fractions of 9.5 Gy using the CyberKnife robotic radiation surgery system (Accuray, Inc, Sunnyvale, CA), emulating high-dose rate (HDR) brachytherapy (14-16). The use of extreme hypofractionation might increase the impact of intrafraction motion, due to longer treatment fraction time and reduced statistical averaging of position errors. Moreover, the use of a simultaneously integrated boost (SIB) to deliver a higher dose to the peripheral zone of the prostate could increase the susceptibility to uncorrected rotations. The effect of intrafraction prostate translations and rotations on these hypofractionated treatments with a SIB has, to our knowledge, not been investigated before.

To correct intrafraction prostate motion, the CyberKnife is equipped with an automated marker tracking system (17). The system acquires orthogonal kV images with a user-defined interval and automatically adjusts the position and orientation of the robotic manipulator or treatment couch during treatment fractions. The system also features an adaptive timing mode in which the time interval between corrections is reduced when large displacements are observed. To account for residual motion between corrections, a planning target volume (PTV) is constructed in our clinic by applying a 3-mm margin around the clinical target volume (CTV) (15,16). The relevance of intrafraction corrections has been reported previously for other hypofractionated treatments (18-21), but the effectiveness of these measures to account for intrafraction prostate motion during CyberKnife treatments has not been investigated before. In relation to this, it has also not been investigated before whether more frequent and more accurate robot corrections would allow for a reduction of the PTV margin.

The aim of this study was to quantify the dosimetric impact of the timing and extent of translational and rotational corrections during hypofractionated CyberKnife treatments and of the applied CTV-to-PTV margins. For this purpose, we performed treatment simulations using different time intervals between corrections, using various degrees of robot corrections and CTV-to-PTV margins of 0 and 3 mm.

## Methods and Materials

### Prostate motion data

Real-time prostate motion data was collected by using an electromagnetic tracking device (Calypso Medical Technologies, provided by the Department of Radiation Oncology of the M.D. Anderson Cancer Center [Orlando, FL]) (5,6). The device measured the position of implanted transponders with a frequency of 10 Hz. A total of 548 prostate motion tracks of 17 patients (denoted by "motion data patients") were at our disposal. The average length of the motion tracks was 10.1 $\pm$ 2.0 min (1 SD). Prostate rotations were not recorded by the tracking device but should also be taken into account to adequately determine the impact of intrafraction motion on the delivered dose (4). Several studies of interfraction prostate motion showed that rotations around the left-right axis are predominant and that prostate motion can be approximated in the sagittal plane by rotations around the apex (1-3). Based on these studies, we derived left-right rotations by converting the anterior-posterior translations into rotations around the prostate apex as shown in Figure 1. Rotations around the anterior-posterior and superior-inferior axes are generally small and were not taken into account in this study.

### Treatment plans

Treatment plans were generated using Erasmus iCycle, a treatment planning system developed in-house (22) that was extended with CyberKnife treatment planning (23,24). The planning system performs "prioritized" optimization, which means that objectives are optimized successively according to their assigned priorities. The constraints and the objectives with their priorities are defined by the user in the so-called wish list. Typically, the same wish list can be used for an entire patient group, thereby allowing for fully automated plan generation (25,26). For CyberKnife treatments using circular aperture collimators, Erasmus iCycle features a node-reduction technique to generate time-efficient treatment plans (23). In this study, we assumed that CyberKnife beam collimation was performed using a variable circular aperture collimator (27).

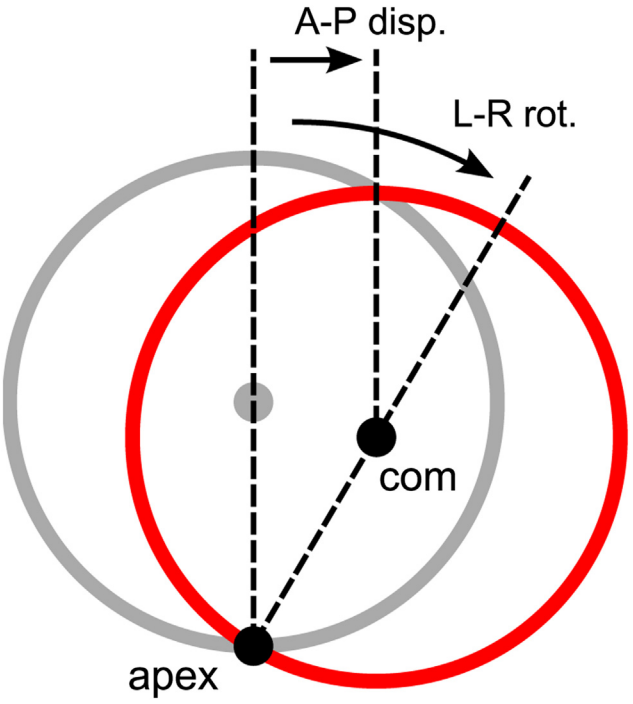


**Fig. 1.** Schematic illustration showing the conversion of center-of-mass (com) displacements (disp.) in anterior-posterior (A-P) direction into rotations (rot.) around the left-right (L-R) axis.

**Table 1** Wish list containing constraints and objectives used for plan generation for the prostate cases in this study

| Constraints | | |
|---|---|---|
| Structure | Type | Limit |
| PTV | Minimum | 0.99 × 38 Gy |
| PTV | Maximum | 1.50 × 38 Gy |
| CTV | Minimum | 1.02 × 38 Gy |
| Peripheral zone | Minimum | 1.19 × 38 Gy |
| PTV-ring 10 mm | Maximum | 30 Gy |
| PTV-ring 20 mm | Maximum | 19 Gy |
| PTV-ring 30 mm | Maximum | 17 Gy |
| Skin | Maximum | 17 Gy |
| Urethra | Maximum | 41 Gy |
| Penis-scrotum | Maximum | 4 Gy |

| Objectives | | | |
|---|---|---|---|
| Priority | Structure | Type | Goal |
| 1 | Rectum | gEUD-12 | 1 Gy |
| 2 | Bladder | gEUD-12 | 1 Gy |
| 3 | Rectal mucosa | gEUD-12 | 1 Gy |
| 4 | Rectum | Mean | 1 Gy |
| 5 | Urethra | Mean | 1 Gy |
| 6 | Bladder | Mean | 1 Gy |
| 7 | Cumulative beam weight | Sum | 1 MU |

*Abbreviations:* CTV = clinical target volume; gEUD-12 = generalized equivalent uniform dose using a biological parameter of 12; MU = monitor unit; PTV = planning target volume.
Priority numbers indicate the order in which the objectives were optimized; a low number corresponds to a high-priority objective. A constraint must always be fulfilled during treatment planning. Dose limits for the targets (PTV, CTV, and peripheral zone) are expressed relative to the prescribed dose (38 Gy).

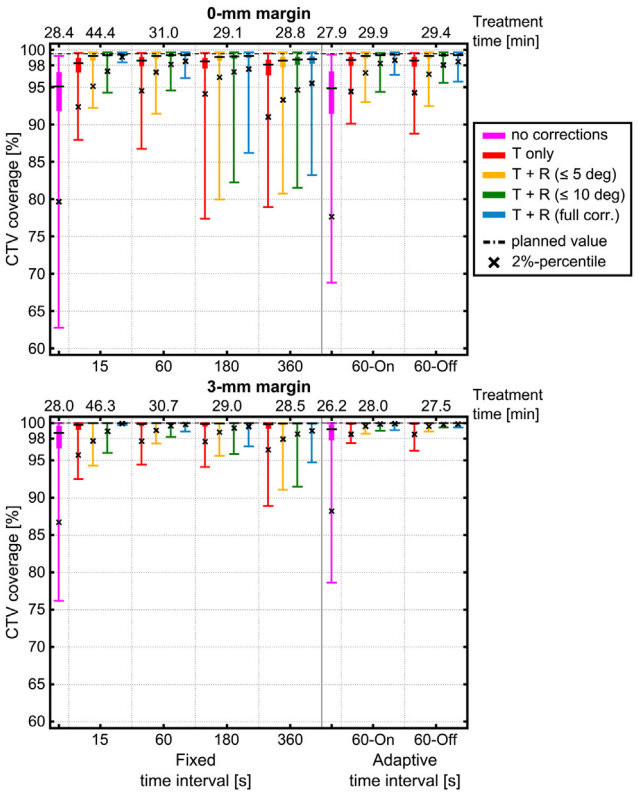


**Fig. 2.** The CTV coverage (volume receiving 100% of the prescribed dose, $V_{100\%}$) of the 0-mm (upper graph) and 3-mm (lower graph) margin plans is shown for different correction strategies. Each box plot indicates the quartiles. Average simulated treatment times are shown for each time interval. CTV = clinical target volume; R = rotational correction; T = translational correction.

Treatment plans were generated for 3 prostate cases, with CTVs ranging from 52 to 66 mL. The CTV consisted of the prostate without seminal vesicles. Treatment planning was performed according to a virtual HDR brachytherapy protocol (14-16). We required at least 95% of the PTV and 99% of the CTV to receive 38 Gy (4 fractions, prescribed at 67% isodose) and at least 95% of the peripheral zone to receive 120% of the prescribed dose (45.6 Gy). Urethra dose was restricted, and doses to surrounding organs-at-risk (OARs) were minimized. The wish list used in this study to achieve these aims is given in Table 1. For each prostate case, treatment plans were generated using 2 CTV-to-PTV margins: the clinically applied margin of 3 mm and a reduced margin of 0 mm. For each margin, 2 treatment plans were generated: 1 using the standard prostate node set and 1 using the adaptive timing prostate node set. A node set contains the principal beam directions from which the CyberKnife can irradiate. The standard prostate node set contains 106 node positions. The adaptive timing node set contains only 72 node positions, as node positions that block the imaging system are left out.

## Treatment simulations

We simulated realistic 4-fraction CyberKnife treatments by combining real-time prostate motion data with the CyberKnife delivery characteristics (ie, robot trajectory and speed, linear accelerator output, and correction strategy). As treatment fractions were longer than the individual motion tracks, available tracks were randomly combined by connecting the end point of one track with the starting point of another track. Only tracks belonging to the same motion data patient were combined, and connection points during beam-on time were not allowed to avoid unrealistic changes in prostate motion. Because the prostate motion data only described intrafraction displacements, we intrinsically simulated perfect patient set up at the start of each treatment fraction. For each treatment fraction, the time points were determined when beams were switched on and off and when imaging and subsequent correction were performed. Imaging was simulated to be performed when the next beam could not be delivered within a user-defined time interval since the last image acquisition. At each imaging/correction time-point, the robot correction was determined according to the simulated correction strategy. The residual motion was then calculated as the difference between the prostate displacements and the applied robot corrections. A detailed description of the combined prostate motion tracks is provided in the Supplementary Material.

Using the residual motion track as input, a 4-dimensional (4D) dose calculation was performed by an algorithm developed in-house. The static dose distribution was calculated (at CT grid resolution) for each beam individually, inside a region of interest enclosing all possible locations and orientations of the CTV and high-dose regions of the OARs. The delivered dose of each beam

**Table 2** Percentage of treatments with at least 98% CTV coverage ($V_{100\%} \geq 98\%$) for different correction strategies and margins*

| Time interval [s] | 0-mm standard plan | | | | | 3-mm standard plan | | | | |
|---|---|---|---|---|---|---|---|---|---|---|
| | No corr. | T only | T+R(≤5°) | T+R(≤10°) | T+R(full) | No corr. | T only | T+R(≤5°) | T+R(≤10°) | T+R(full) |
| no imaging | 11.2 | - | - | - | - | 61.0 | - | - | - | - |
| 15 | - | 56.6 | 84.8 | 94.9 | 100.0 | - | 90.3 | 96.9 | 99.1 | 100.0 |
| 60 | - | 70.1 | 92.2 | 98.4 | 99.5 | - | 96.6 | 99.7 | 100.0 | 100.0 |
| 180 | - | 64.6 | 87.4 | 94.0 | 95.8 | - | 95.8 | 99.6 | 99.8 | 99.9 |
| 360 | - | 51.5 | 68.3 | 74.4 | 78.9 | - | 91.1 | 97.7 | 99.2 | 99.6 |

≥98%
≥95% and <98%
≥90% and <95%
<90%

| | 0-mm adaptive plan | | | | | 3-mm adaptive plan | | | | |
|---|---|---|---|---|---|---|---|---|---|---|
| | No corr. | T only | T+R(≤5°) | T+R(≤10°) | T+R(full) | No corr. | T only | T+R(≤5°) | T+R(≤10°) | T+R(full) |
| no imaging | 12.8 | - | - | - | - | 71.3 | - | - | - | - |
| 60-On | - | 71.6 | 93.4 | 98.7 | 99.8 | - | 99.5 | 100.0 | 100.0 | 100.0 |
| 60-Off | - | 68.5 | 91.5 | 98.0 | 99.5 | - | 99.4 | 100.0 | 100.0 | 100.0 |

*Abbreviations:* R = rotational corrections; T = translational corrections; 60-On = initial time interval of 60 seconds with adaptive timing switched on; 60-Off = initial time interval of 60 seconds with adaptive timing switched off.

* When the percentage of treatments is higher than 98%, the correction strategy is displayed in green, between 95% and 98% in yellow, between 90% and 95% in orange, and lower than 90% in red. A color version of this figure is available at www.redjournal.org.

was then obtained by convoluting the static dose with the residual motion track corresponding to the beam-on-time. The residual motion tracks were down-sampled to 1 data point per 5 seconds, as this provided a reasonable tradeoff between calculation time and simulation accuracy. The total dose distribution was subsequently calculated by adding the convoluted dose distributions of all beams for all 4 treatment fractions.

For the standard treatment plans, simulations were performed using fixed time intervals between corrections of 15, 60, 180, and 360 seconds. For the adaptive timing treatment plans, simulations were performed with the adaptive timing mode both switched on and off. During adaptive imaging/correction, the time interval was reduced from 60 seconds to 15 seconds when translations larger than 3 mm or rotations larger than 2° were observed between 2 consecutive images. For all 6 timing strategies (15, 60, 180, and 360 seconds; adaptive imaging on and adaptive imaging off), 4 different robot correction scenarios were simulated: (*1*) full translational corrections only, and full translational corrections together with rotational corrections up to (*2*) 5°; (*3*) 10°; and (*4*) also fully corrected. Rotational corrections of 5° and 10° corresponded to clinical scenarios in which maximum robot rotational corrections (5°) and an additional maximum robotic couch rotation (5°), respectively, were applied. Treatment simulations were additionally performed for the standard and adaptive timing treatment plans assuming no robot corrections and no image acquisition accordingly. For all 3 prostate cases, 52 combinations of time interval, correction strategy, and margin were simulated. For each combination, we simulated 50 complete 4-fraction treatments for all 17 motion data patients, resulting in a total of 132,600 treatment simulations.

## Evaluation

The dosimetric parameters used for target evaluation were the CTV coverage (volume receiving the prescribed dose, $V_{100\%}$) and the dose received by 98% of the peripheral zone volume (PZ $D_{98\%}$). For the rectum and bladder, the dose received by 1 cc ($D_{1cc}$) was evaluated. The urethra dose was assessed using the dose received by 5% ($D_{5\%}$) and 10% ($D_{10\%}$) of the volume. The near-minimum dose received by the CTV (CTV $D_{98\%}$) is reported in the Supplementary Material.

We evaluated the percentage of treatments for which the CTV coverage was higher than 98%. The correction strategy and margin were considered effective when this requirement was achieved in at least 98% of the treatments. Statistical analysis was performed comparing planned and simulated dose parameters (Wilcoxon signed-rank test), and differences between correction strategies and margins (Wilcoxon rank-sum test). $P$ values less than .05 were considered statistically significant.

## Results

Figure 2 shows the CTV coverage of the 0-mm and 3-mm margin plans for the different correction strategies simulated. Each box plot displays quartiles of the outcomes of 2550 treatment simulations (ie, 3 prostate cases, 17 prostate motion patients, 50 simulations). For the standard 0-mm margin plans, the CTV coverage decreased from the average planned value of 99.5% to 93.6% (SD = 4.8%; range = 62.9%-99.2%; $P<.001$) when no motion correction was applied. The standard 3-mm margin plans were found to be more robust against intrafraction prostate motion, resulting in the CTV coverage decreasing from the average planned value of 100% to 97.4% (SD = 3.4%; range = 76.2%-100%; $P<.001$) when no motion correction was applied. The CTV coverage was better preserved with increasing extents of robot corrections and in general for shorter time intervals between corrections. However, the beneficial effect of reducing time intervals was marginal for intervals smaller than 60 to 180 seconds. The effect of enabling or disabling adaptive timing (ie, allowing it to switch to a 15-second time interval in case of large prostate displacements) was found to be very small, but the 3-mm adaptive timing plans were less sensitive than the standard treatment plans.

Percentages of treatments with more than 98% CTV coverage are listed in Table 2. For the 0-mm margin plans, this requirement was met in more than 98% of treatments when applying translational corrections and rotational corrections up to 10° (or more), using a time interval of 60 seconds. Translational corrections and

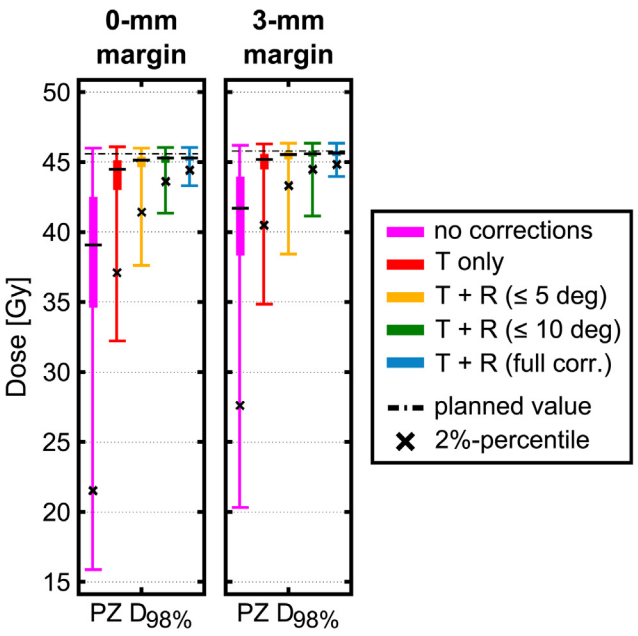


**Fig. 3.** The dose received by 98% of peripheral zone (PZ $D_{98\%}$) is shown for the 0-mm (left graph) and 3-mm (right graph) margin plans and for different correction strategies, using a time interval of 60 seconds. Each box plot indicates quartiles. R = rotational corrections; T = translational corrections.

rotational corrections up to 5° (or more) together with a time interval of 60 seconds or 180 seconds were required for the standard 3-mm margin plans to achieve similar CTV coverage in at least 98% of the treatments.

Figure 3 shows the effect of intrafraction prostate motion on the boost dose in the PZ when using a time interval of 60 seconds. The $D_{98\%}$ of the PZ decreased significantly for both CTV-to-PTV margins, when no motion correction was applied, from an average planned value of 45.6 Gy to a simulated value of 37.7 Gy (SD = 6.0 Gy; range = 15.9-46.0 Gy; $P<.001$) for the 0-mm margin plans and from 45.8 Gy to 40.4 Gy (SD = 4.6 Gy; range = 20.3-46.2 Gy; $P<.001$) for the 3-mm margin plans. Translational and rotational corrections should be applied for both CTV-to-PTV margins when the $D_{98\%}$ is required to be, for example, at least 110% of the prescribed dose in more than 98% of the treatments.

The dose received by the OARs when using a time interval of 60 seconds is shown in Figure 4 for the 3 prostate cases separately. OAR doses were generally found to increase due to uncorrected intrafraction motion and to be better preserved with increasing extents of robot corrections. However, rectum $D_{1cc}$ values decreased due to uncorrected motion by, on average, $-1.9 \pm 5.5$ Gy (1 SD) for the 0-mm plans and by $-3.4 \pm 5.4$ Gy for the 3-mm plans. The prostate tended to move dorsally in the prostate motion data, and the rectum was simulated to displace accordingly, thereby moving into a region with lower doses. For the rectum and bladder, planned $D_{1cc}$ values were lower in the 0-mm margin plans than in the 3-mm margin plans by, on average, 6.8 Gy (range = 4.0-9.0 Gy) and 5.2 Gy (range = 4.1-5.9 Gy), respectively. As a result, rectum and bladder sparing were found to be considerably better for the 0-mm margin plans. When using the correction strategies to achieve 98% CTV coverage in at least 98% of treatments, rectum doses differed from the planned values by, on average, $0.1 \pm 3.0$ Gy and $-0.2 \pm 1.2$ Gy for the 0-mm and 3-mm margin plans, respectively, whereas bladder $D_{1cc}$ values differed by, on average, $0.3 \pm 1.9$ Gy and $0.4 \pm 1.2$ Gy, respectively. The effect of intrafraction prostate motion on urethra dose was generally small.

## Discussion

In this study, the actual delivered dose in the presence of intrafraction motion was simulated for hypofractionated CyberKnife prostate treatments with a SIB. To achieve the 98% CTV coverage in at least 98% of the treatments, rotational corrections of up to 10° and up to 5° (in addition to full translational corrections) were required for a 0-mm and 3-mm margin, respectively. This requirement may be perceived as very strict but is in line with the excellent treatment outcomes that should be considered standard in this patient group (28). It is important to note that other treatment uncertainties (eg, beam delivery inaccuracy and delineation uncertainty) were not considered in the current study and that additional margins should be applied to account for these treatment uncertainties.

An important finding of the current study is the fact that more frequent imaging/correction (eg, 15-second time interval) does not necessarily result in improved CTV coverage. As image acquisition and correction take time, the fraction duration increased with a decreasing time interval (Fig. 2), which resulted in larger residual errors when displacements were not fully corrected (see Supplementary Material). This might also explain the improved robustness of the 3-mm adaptive timing plans, which had considerably shorter treatment times than the standard treatment plans. The optimal time interval and to what extent it can further improve the delivered dose should be established in future research. Xie et al (7) performed a geometrical analysis and advised a time interval of approximately 40 seconds, which is considerably shorter than 60 to 180 seconds recommended in this study. The current study shows that short time intervals should be used with caution.

Prostate motion data measured by the Calypso system was previously used to perform a dosimetric evaluation of helical tomotherapy (HT) and step-and-shoot intensity modulated radiation therapy (IMRT) (11, 12). In contrast to the findings in the current study, the effect of intrafraction motion was concluded to be generally low for both delivery techniques. This is probably due to the fact that these studies only included prostate translations and due to the use of larger PTV margins (5 mm, 3 mm in posterior direction), homogeneous dose distributions and 2-Gy fractions in HT and IMRT treatments. Whether the findings of the current study also hold for hypofractionated prostate treatments delivered using different treatment machines, but with a similar SIB scheme and tight margins, should be established in future studies.

We used CT data from 3 prostate cancer patients previously treated in our clinic using the CyberKnife, as the CT data corresponding to the Calypso motion tracks were not at our disposal. Correlation between patient anatomy and prostate motion was therefore missing. Although rectum and bladder doses varied considerably (Fig. 4), we observed very similar patterns for the CTV dose for all 3 patients. Based on these results, we speculate that the findings of the current study also hold for other patients.

In the current study, rotations around the left-right axis were derived from the measured anterior-posterior translations, and we randomly combined motion tracks to obtain tracks of sufficient length. These operations might have introduced errors compared

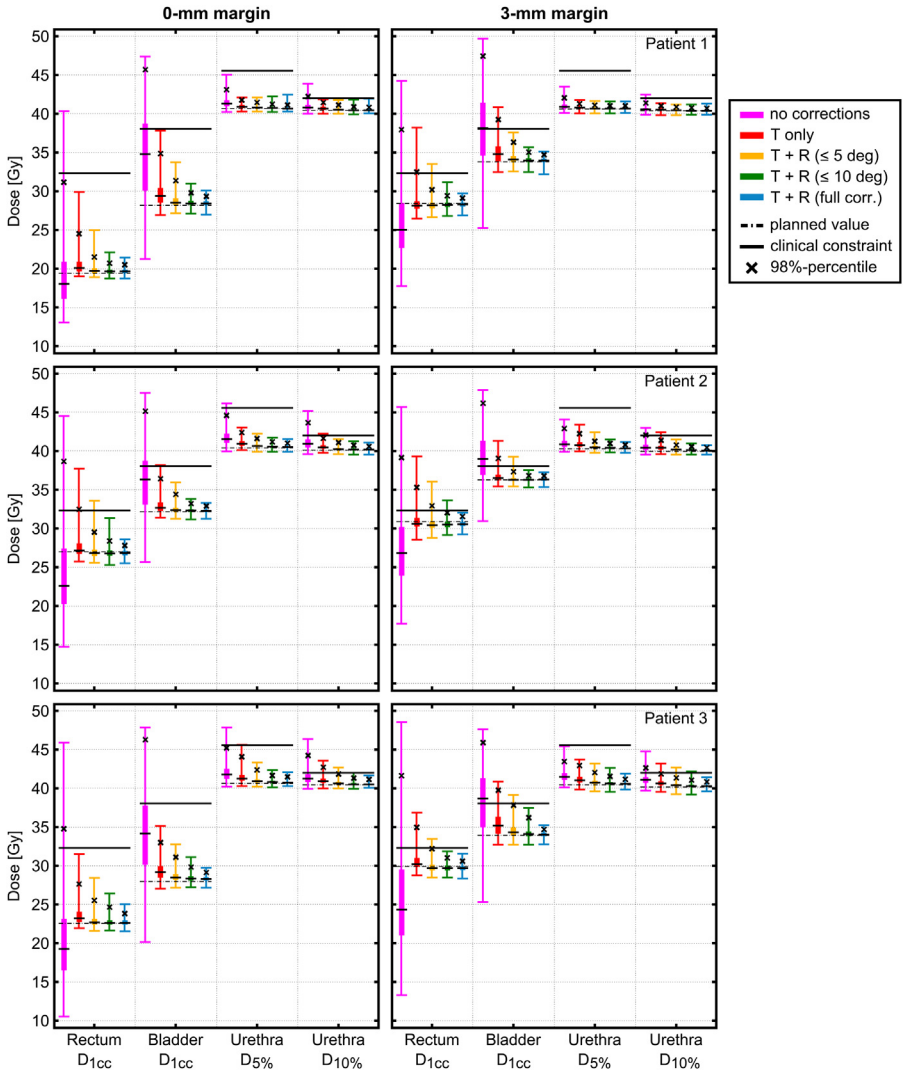


**Fig. 4.** OAR dose parameters of the 0-mm (left column) and 3-mm (right column) margin plans of the individual prostate cases (rows) are shown for different correction strategies, using a time interval of 60 seconds. Each box plot indicates quartiles. OAR = organs at risk; R = rotational correction; T = translational correction.

with actual prostate motion during a CyberKnife treatment fraction. This is, however, difficult to verify, as intrafraction motion data for fractions of comparable length are not reported in the literature. A detailed description of the simulated prostate motion is provided in the Supplementary Material, which can be used for comparison and to relate the outcomes of this study to CyberKnife treatments at other institutes. A further limitation of this study is the assumption of rigid organ motion, which can be realistically assumed for the prostate (without vesicles) and urethra, but is likely to be inadequate for the rectum and bladder. However, as the high-dose regions in these organs are located very close to the prostate, rigid motion seems a reasonable assumption for the $D_{1cc}$-parameter that we evaluated. Finally, we assumed the densities encountered by each beam along its path to be constant during the entire treatment.

## Conclusions

For hypofractionated CyberKnife prostate treatments with a simultaneously integrated boost, intrafraction motion can have a substantial impact on doses delivered to the CTV, boost volume, rectum, and bladder. Applying robot corrections with a time interval of 60 to 180 seconds was found to be an effective way to account for prostate motion. To ensure 98% CTV coverage in more than 98% of the treatments, translational and rotational corrections up to 10° are recommended when using a 0-mm margin, while rotational corrections up to 5° are advised when using a 3-mm margin. Rectum and bladder were spared considerably better by using a 0-mm margin. The adaptive time interval feature did not improve delivered dose distributions.

## References

1. Van Herk M, Bruce A, Guus Kroes AP, et al. Quantification of organ motion during conformal radiotherapy of the prostate by three dimensional image registration. *Int J Radiat Oncol Biol Phys* 1995;33:1311-1320.
2. Hoogeman MS, van Herk M, de Bois J, et al. Strategies to reduce the systematic error due to tumor and rectum motion in radiotherapy of prostate cancer. *Radiother Oncol* 2005;74:177-185.

3. de Boer HC, van Os MJ, Jansen PP, et al. Application of the no action level (NAL) protocol to correct for prostate motion based on electronic portal imaging of implanted markers. *Int J Radiat Oncol Biol Phys* 2005;61:969-983.
4. Aubry JF, Beaulieu L, Girouard LM, et al. Measurements of intrafraction motion and interfraction and intrafraction rotation of prostate by three-dimensional analysis of daily portal imaging with radiopaque markers. *Int J Radiat Oncol Biol Phys* 2004;60:30-39.
5. Kupelian P, Willoughby T, Mahadevan A, et al. Multi-institutional clinical experience with the Calypso System in localization and continuous, real-time monitoring of the prostate gland during external radiotherapy. *Int J Radiat Oncol Biol Phys* 2007;67:1088-1098.
6. Langen KM, Willoughby TR, Meeks SL, et al. Observations on real-time prostate gland motion using electromagnetic tracking. *Int J Radiat Oncol Biol Phys* 2008;71:1084-1090.
7. Xie Y, Djajaputra D, King CR, et al. Intrafractional motion of the prostate during hypofractionated radiotherapy. *Int J Radiat Oncol Biol Phys* 2008;72:236-246.
8. Mutanga TF, de Boer HCJ, Rajan V, et al. Day-to-day reproducibility of prostate intrafraction motion assessed by multiple kV and MV imaging of implanted markers during treatment. *Int J Radiat Oncol Biol Phys* 2012;83:400-407.
9. Deutschmann H, Kametriser G, Steininger P, et al. First clinical release of an online, adaptive, aperture-based image-guided radiotherapy strategy in intensity-modulated radiotherapy to correct for inter- and intrafractional rotations of the prostate. *Int J Radiat Oncol Biol Phys* 2012;83:1624-1632.
10. Lin Y, Liu T, Yang W, et al. The non-Gaussian nature of prostate motion based on real-time intrafraction tracking. *Int J Radiat Oncol Biol Phys* 2013;87:363-369.
11. Langen KM, Lu W, Willoughby TR, et al. Dosimetric effect of prostate motion during helical tomotherapy. *Int J Radiat Oncol Biol Phys* 2009;74:1134-1142.
12. Langen KM, Chauhan B, Siebers JV, et al. The dosimetric effect of intrafraction prostate motion on step-and-shoot intensity-modulated radiation therapy plans: Magnitude, correlation with motion parameters, and comparison with helical tomotherapy plans. *Int J Radiat Oncol Biol Phys* 2012;84:1220-1225.
13. Mutanga TF, de Boer HC, Rajan V, et al. Software-controlled, highly automated intrafraction prostate motion correction with intrafraction stereographic targeting: System description and clinical results. *Med Phys* 2012;39:1314-1321.
14. Fuller DB, Naitoh J, Lee C, et al. Virtual HDRSM CyberKnife treatment for localized prostatic carcinoma: Dosimetry comparison with HDR brachytherapy and preliminary clinical observations. *Int J Radiat Oncol Biol Phys* 2008;70:1588-1597.
15. Aluwini S, van Rooij P, Hoogeman M, et al. CyberKnife stereotactic radiotherapy as monotherapy for low- to intermediate-stage prostate cancer: Early experience, feasibility, and tolerance. *J Endourol* 2010;24:865-869.
16. Aluwini S, van Rooij P, Hoogeman M, et al. Stereotactic body radiotherapy with a focal boost to the MRI-visible tumor as monotherapy for low- and intermediate-risk prostate cancer: Early results. *Radiat Oncol* 2013;8:1-7.
17. Kilby W, Dooley JR, Kuduvalli G, et al. The CyberKnife robotic radiosurgery system in 2010. *Technol Cancer Res Treat* 2010;9:433-452.
18. Hoogeman MS, Nuyttens JJ, Levendag PC, et al. Time dependence of intrafraction patient motion assessed by repeat stereoscopic imaging. *Int J Radiat Oncol Biol Phys* 2008;70:609-618.
19. Murphy MJ. Intrafraction geometric uncertainties in frameless image-guided radiosurgery. *Int J Radiat Oncol Biol Phys* 2009;73:1364-1368.
20. Gevaert T, Boussaer M, Engels B, et al. Evaluation of the clinical usefulness for using verification images during frameless radiosurgery. *Radiother Oncol* 2013;108:114-117.
21. Kang KM, Chai GY, Jeong BK, et al. Estimation of optimal margin for intrafraction movements during frameless brain radiosurgery. *Med Phys* 2013;40:051716.
22. Breedveld S, Storchi PRM, Voet PWJ, et al. iCycle: Integrated, multicriterial beam angle, and profile optimization for generation of coplanar and noncoplanar IMRT plans. *Med. Phys* 2012;39:951-963.
23. Van de Water S, Hoogeman MS, Breedveld S, et al. Shortening treatment time in robotic radiosurgery using a novel node reduction technique. *Med. Phys* 2011;38:1397-1405.
24. Van de Water S, Hoogeman MS, Breedveld S, et al. Variable circular collimator in robotic radiosurgery: a time-efficient alternative to a mini-multileaf collimator? *Int. J. Radiat. Oncol. Biol. Phys* 2011;81:863-870.
25. Rossi L, Breedveld S, Heijmen BJM, et al. On the beam direction search space in computerized non-coplanar beam angle optimization for IMRT-prostate SBRT. *Phys. Med. Biol.* 2012;57:5441.
26. Voet PWJ, Dirkx MLP, Breedveld S, et al. Toward Fully Automated Multicriterial Plan Generation: A Prospective Clinical Study. *Int. J. Radiat. Oncol. Biol. Phys.* 2013;85:866-872.
27. Echner GG, Kilby W, Lee M, et al. The design, physical properties and clinical utility of an iris collimator for robotic radiosurgery. *Phys Med Biol* 2009;54:5359-5380.
28. Demanes DJ, Martinez AA, Ghilezan M, et al. High-dose-rate monotherapy: Safe and effective brachytherapy for patients with localized prostate cancer. *Int J Radiat Oncol Biol Phys* 2011;81:1286-1292.